RMetS
Royal Meteorological Society

The impact of the AMO on the West African monsoon annual cycle

Elinor R. Martin* Chris D. Thorncroft

Department of Atmospheric and Environmental Sciences, University at Albany, SUNY, NY, USA

*Correspondence to: Elinor R. Martin, DAES-ES351, Department of Atmospheric and Environmental Sciences, University at Albany, 12222 Albany, NY, United States. E-mail: emartin4@albany.edu

A combination of observations and re-analysis was used to investigate the mechanisms of the connection between the Atlantic Multidecadal Oscillation (AMO) and Sahel rainfall. A composite technique based on the AMO index was used to identify differences between warm and cold phases of the AMO. A significant summer rainfall increase over the Sahel during warm phases of the AMO was observed, with large increases during the typical monsoon onset period in June. In spring of warm phases of the AMO prior to monsoon onset, strengthening of the Saharan heat-low and its associated shallow meridional overturning circulation is observed. The intensified shallow meridional overturning circulation increases moisture flux into the Sahel from the south during spring while increased westerly winds from the Atlantic increase westerly moisture flux into the Sahel during spring and summer. The strengthening of the heat-low is accompanied by increases in Mediterranean sea-surface temperatures during warm phases of the AMO that lead to increases in moisture flux convergence in the northeast Sahel. During warm phases of the AMO the African easterly jet is farther north than in cold phases, and increased African easterly wave (AEW) activity across West Africa and into the Atlantic is observed. This increased AEW activity particularly in the early hurricane season, as measured by eddy kinetic energy, may be contributing to the increased number of Atlantic tropical storms during warm phases of the AMO. Copyright © 2013 Royal Meteorological Society

Key Words: AMO; Sahel; rainfall; AEWs; heat-low

Received 15 May 2012; Revised 14 December 2012; Accepted 19 December 2012; Published online in Wiley Online Library

Citation: Martin ER, Thorncroft CD. 2013. The impact of the AMO on the West African monsoon annual cycle. *Q. J. R. Meteorol. Soc.* DOI:10.1002/qj.2107

1. Introduction

Sahel precipitation is well known to have undergone large multidecadal variability over the past century (Figure 1), with wet conditions in the 1940s and 1950s and a switch to dry conditions in the 1960s. Multidecadal variability in Sahelian rainfall has been attributed to variability in sea-surface temperature (SST) in the Atlantic (Lamb, 1978a, 1978b; Folland *et al.*, 1986; Hastenrath, 1990; Rowell *et al.*, 1995; Ward, 1998; Knight *et al.*, 2006; Zhang and Delworth, 2006; Ting *et al.*, 2009), Indian and Pacific Oceans (Bader and Latif, 2003; Giannini *et al.*, 2003; Biasutti *et al.*, 2008; Lu, 2009; Caminade and Terray, 2010; Mohino *et al.*, 2011; Rodríguez-Fonseca *et al.*, 2011). Persistent Sahel drought connected to changes in Atlantic SSTs has even been documented in palaeoclimate records over the past three millennia (Shanahan *et al.*, 2009). These sustained wet and dry periods have large economic and societal impacts in the region, making them important to understand, represent in climate model simulations, and ultimately predict.

The Atlantic Multidecadal Oscillation (AMO) is a coherent multidecadal variation of SSTs over the North Atlantic, including the tropical North Atlantic. Cold AMO phases (cold SSTs over the entire North Atlantic) have been

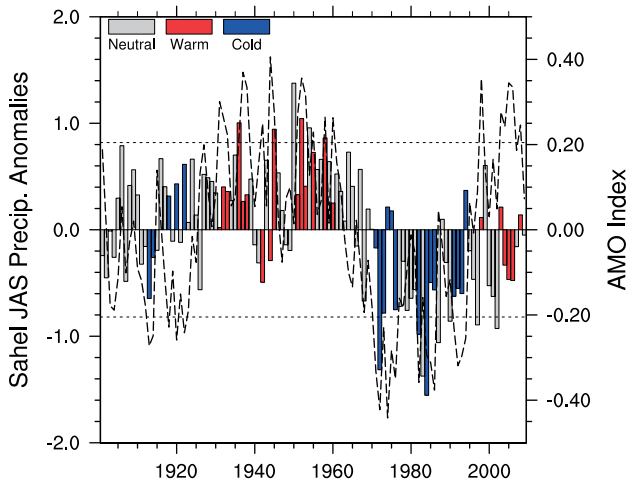

Figure 1. Time series of summer (JAS) Sahel (10°N–20°N, 20°W–10°E) precipitation anomalies (mm day^{-1}, left axis, bars) and the AMO index (°C, right, dashed line). Dotted lines are +/− one standard deviation of AMO. Coloured bars indicate years when the AMO was in the warm or cold phase. This figure is available in colour online at wileyonlinelibrary.com/journal/qj

observed in the early 1900s and the 1960s–1980s with the warm AMO phase observed in the 1930s–1950s and early 2000s, as shown in Figure 1. The warm (or positive) phase of the AMO has been shown to coincide with increased summer rainfall over the Sahel due to a northward displacement of the intertropical convergence zone (ITCZ) (Folland *et al.*, 1986; Rowell *et al.*, 1995; Knight *et al.*, 2006; Zhang and Delworth, 2006; Ting *et al.*, 2009) as well as increased hurricane formation and decreased northeast Brazil rainfall (Knight *et al.*, 2006).

The multidecadal variability of North Atlantic SSTs has been attributed to internal ocean circulation changes, such as changes in the Atlantic meridional overturning circulation (Kerr, 2000; Knight *et al.*, 2005; Ting *et al.*, 2009). Recently, more attention has been placed on the role of aerosols (both anthropogenic and natural) in controlling SST temperature gradients in the Atlantic on decadal and longer time-scales (Ackerley *et al.*, 2011; Booth *et al.*, 2012). Although this study will focus on the response to multidecadally varying SSTs rather than the cause, it is important to note the recent discussion in the literature regarding how much of the multidecadal SST signal is driven by internal ocean dynamics versus aerosol-driven impacts.

Climate model experiments, along with observations, have been used to show the importance of the AMO in controlling multidecadal fluctuations of Sahel and West African rainfall. The first low-frequency mode of summer Sahel rainfall has been shown to be associated with the AMO SST pattern in the Atlantic (Zhang and Delworth, 2006; Mohino *et al.*, 2011; Rodríguez-Fonseca *et al.*, 2011). The first empirical orthogonal function (EOF) of low-frequency Sahel summer rainfall also matches closely with the regression of the low-frequency rainfall on the AMO index, again suggesting the importance of the AMO in the low-frequency variability of Sahel rainfall (Zhang and Delworth, 2006). Mohino *et al.* (2011) used climate model experiments to show that the switch to the cold phase of the AMO in the 1980s could explain 50% of the SST-driven Sahel reduction in rainfall, thus highlighting the importance of understanding the connection between the AMO and Sahel rainfall.

Early studies of decadal changes in Sahel rainfall showed that cooling of the tropical North Atlantic was accompanied by a surface pressure rise, strengthening of trade winds and southward displacement of the ITCZ in the summer leading to a reduction of Sahel rainfall (Lamb, 1978a, 1978b; Hastenrath, 1990). More recent studies have invoked the role of low-level onshore westerly winds, displacement of the African easterly jet (AEJ) and changes in shear instabilities to changes in summer Sahel rainfall between the wet and dry periods (Grist and Nicholson, 2001; Nicholson and Grist, 2001; Wang and Gillies, 2011) while Hastenrath and Polzin (2011) emphasize the importance of tropical Atlantic SST in variations of Sahelian rainfall through changes in sea-level pressure (SLP) and cross-equatorial winds.

Emphasis in previous studies has been placed on summer rainfall changes in the Sahel, which is when the Sahel receives its climatological maximum in rainfall. Ward (1998) shows that, on decadal time-scales, the increase in Sahel rainfall during the summer tends to migrate meridionally with the annual cycle, indicating that the AMO may impact the entire annual cycle in West Africa, potentially having large impacts for agriculture in the region. Hence, more work is needed to improve our understanding of the influence of the AMO on the complete annual cycle.

The annual cycle of West African monsoon (WAM) rainfall is characterized by four key phases: oceanic (November–mid-April), coastal (mid-April–June), transitional (first half of July) and Sahelian (mid-July–September) (Thorncroft *et al.*, 2011). Although the structure is well observed, prediction and understanding of the mechanisms controlling the annual cycle and the shift in the location of the peak rainfall in particular are still challenging (Sultan and Janicot, 2003; Cook and Vizy, 2006; Hagos and Cook, 2007). Two key features associated with the annual cycle of the WAM are the Atlantic cold tongue in the Gulf of Guinea and the Saharan heat-low (and its associated shallow meridional circulation) (Sultan and Janicot, 2003; Hagos and Cook, 2007; Thorncroft *et al.*, 2011). The influence of the AMO on these features will be investigated.

This article aims to identify and investigate how changes in Atlantic SST associated with the AMO influence the annual cycle of the WAM on decadal time-scales. We aim to assess whether previously proposed mechanisms of Sahel rainfall decadal variability are active in the AMO–WAM decadal-scale variability, and whether other mechanisms (e.g. Gulf of Guinea SSTs and Saharan heat-low strength) are playing an important role. We aim to assess these mechanisms throughout the annual cycle.

2. Data and methodology

A combination of monthly observational data and re-analysis is used to investigate the mechanisms connecting the AMO and Sahel rainfall. The Hadley Centre global sea-Ice and Sea-Surface Temperature (HadISST) dataset is used for global SSTs at 1° horizontal resolution from 1901 through to 2009 and is a blended dataset of both *in situ* and satellite estimates (Rayner *et al.*, 2003). Rainfall estimates are from two different datasets. The Climate Research Unit (CRU) 3.1 precipitation dataset provides long-term land-only monthly data at 0.5° horizontal resolution for 1901–2009 (Mitchell and Jones, 2005). Despite the long period for the CRU dataset, it provides no information over the ocean. Additional rainfall data are from the

Table 1. Number of years identified as in the warm or cold AMO phase for different datasets.

Dataset	Years	Warm AMO	Cold AMO
CRU	1901–2009	21	19
HadISST	1901–2009	21	19
GPCP	1979–2009	6	8
NCEP/NCAR	1948–2009	12	14

Global Precipitation Climatology Project (GPCP), version 2 monthly 2.5° horizontal resolution from 1979 through to 2009 (Adler *et al.*, 2003). The GPCP dataset is a blended product consisting of *in situ* measurements and satellite data and thus provides data over the ocean. In addition to rainfall and SST, other atmospheric variables are provided by the NCEP/NCAR re-analysis dataset (Kalnay *et al.*, 1996) at 2.5° horizontal resolution from 1948 through to 2009. This re-analysis has been chosen due to its long time period, symmetry between the numbers of warm and cold AMO years (Table 1) and agreement in rainfall differences between warm and cold AMO years in the re-analysis and observations. Results with other re-analysis datasets show consistent although not identical results in the large-scale patterns, supporting the use of this product (not shown).

An index of the AMO is calculated following Enfield *et al.* (2001). Monthly SSTs are area-averaged over 0°N–70°N and 10°W–75°W (the North Atlantic) and then detrended. The annually averaged index is shown as the dashed line in Figure 1. A clear decadal signal is apparent (even without time filtering or smoothing), with warm conditions between approximately 1930 and 1960 and cold conditions between 1960 and 2000, with a return to warm conditions since 2000. In order to investigate the impact of the AMO on the WAM, a compositing approach based on warm and cold AMO phases is used, which can be used to compare with results from compositing based on wet and dry years in previous work (Grist and Nicholson, 2001; Nicholson and Grist, 2001; Grist, 2002). Years corresponding to a warm (cold) AMO phase were chosen if the annually averaged AMO index was greater than one standard deviation above (below) the long-term mean. Figure 1 also shows annual Sahel (10°N–20°N, 20°W–10°E) rainfall from the CRU dataset. Sahel rainfall in years corresponding to warm (cold) AMO phases is highlighted red (blue). It is seen that the Sahel is not always wet during warm AMO phases, as other time-scales of variability (such as interannual variability from El Niño/Southern Oscillation events) can dominate decadal variability.

In order to highlight the level of consistency between the longer (but land only) CRU observations and the global lower-resolution GPCP data, the annual cycles of the Sahel rainfall in warm and cold years are compared. The difference between the monthly mean Sahel rainfall amounts in warm and cold years is presented in Figure 2 as a percentage of the annual mean of either GPCP or CRU data. Despite the two datasets containing different numbers of warm and cold AMO phases (as shown in Table 1) and the resolution differences, a consistent annual cycle difference pattern and magnitude emerges from the two products. The CRU data produces a smoother annual cycle of the rainfall difference due to the larger number of years used in the composite analysis. Rainfall differences first emerge in May and rapidly increase to almost 20% of the annual mean in June. Differences maximize in August when the difference between warm and cold years is 50% of the annual mean Sahel rainfall (and 20% of the August mean Sahel rainfall). The difference declines more rapidly after August, reducing to 10% of the annual mean by October. From Figure 2 it is interesting to note that the AMO has a significant impact on rainfall in June, suggesting that the timing of the monsoon onset might be impacted, which will be examined further in section 4. The GPCP data show weak drying in months outside the main monsoon season while CRU shows no change or rainfall increases; however, neither result is significant.

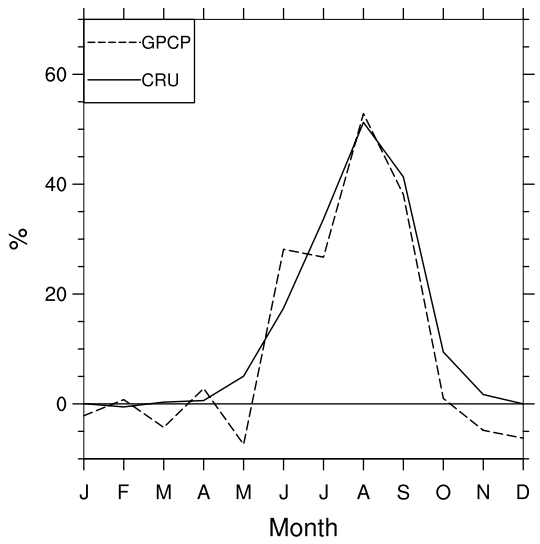

Figure 2. Annual cycle of difference (as percentage of the annual mean) in Sahel (10°N–20°N, 20°W–10°E) precipitation (mm day^{-1}) between warm and cold AMO phases for GPCP and CRU observations.

3. Observed seasonal means

3.1. Sea-surface temperature

Maps showing SST differences between warm and cold phases of the AMO are shown in Figure 3 for four seasons from January to December (JFM, AMJ, JAS and OND). During warm phases of the AMO, warmer SSTs are observed all year in the Atlantic, with the well-known horseshoe pattern evident in each season. These maps of the AMO pattern match well with previous studies of the AMO (e.g. Enfield *et al.*, 2001). There are three main regions of SST changes (all are warmer during the warm AMO phase) that are likely to influence the Sahel rainfall: Gulf of Guinea, Mediterranean Sea and the tropical North Atlantic. The largest changes in SSTs associated with the warm and cold phases of the AMO are confined to the North Atlantic Ocean and Mediterranean Sea (beginning in spring). It is important to note that changes in SSTs between warm and cold AMO years are mainly confined to the Atlantic and Mediterranean, and that differences are not observed in the Indian Ocean and are only small in the Pacific (not shown). Although this compositing method primarily isolates changes in Atlantic SSTs it is likely that there will be an influence from other ocean basins.

Sea-surface temperatures in the Gulf of Guinea are well known to impact both the annual cycle of Sahel rainfall and Sahel rainfall on interannual time-scales (Vizy and Cook,

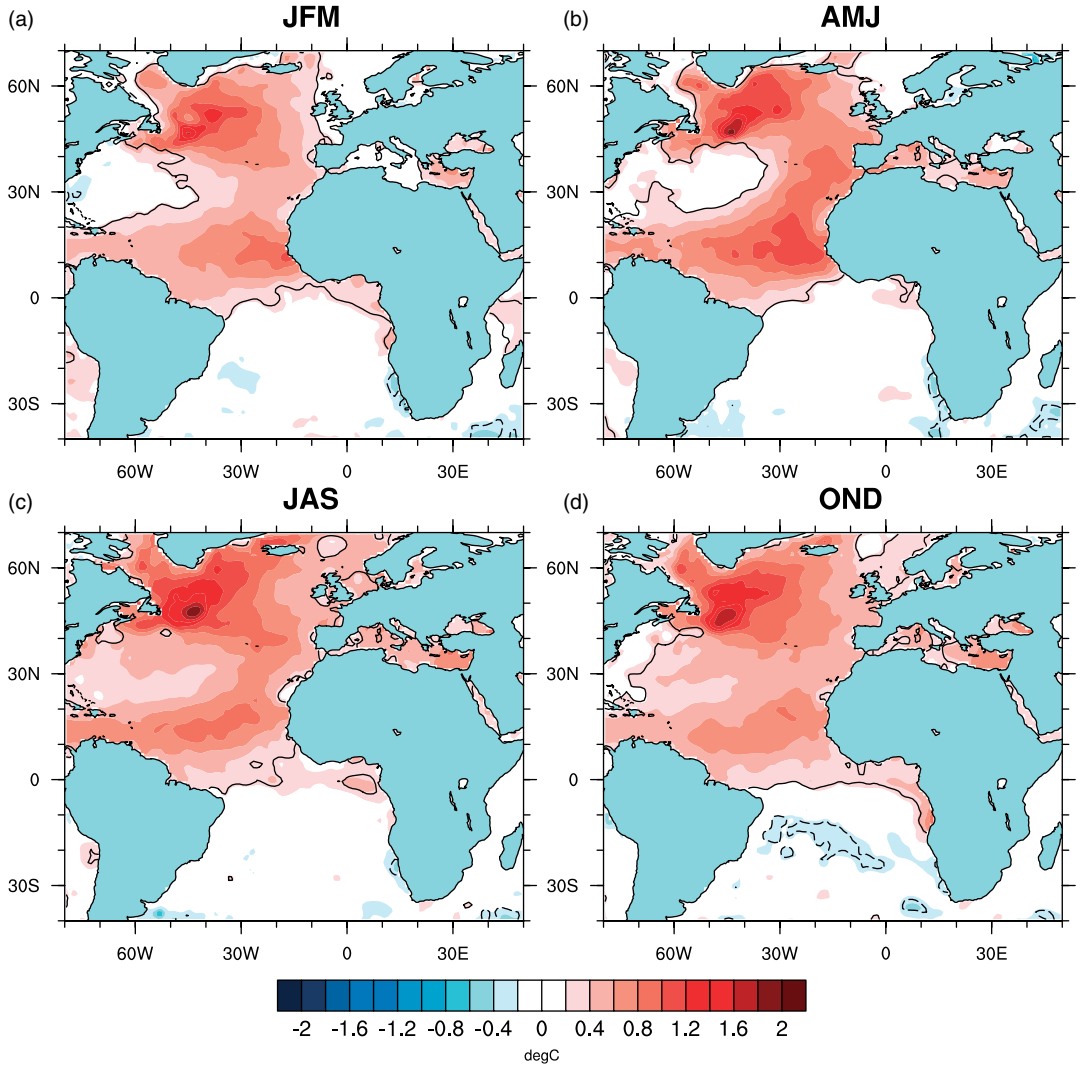

Figure 3. Difference in SST (°C) between warm and cold AMO phases for (a) JFM, (b) AMJ, (c) JAS and (d) OND from HadISST (1901–2009). Black lines indicate regions where SST in warm AMO and cold AMO years are statistically different from each other at the 95% confidence level using a simple Student's *t*-test. Solid lines indicate significant positive differences and dashed lines show significant negative differences. This figure is available in colour online at wileyonlinelibrary.com/journal/qj

2002; Okumura and Xie, 2004; Nicholson and Webster, 2007; Joly and Voldoire, 2010). Warmer Gulf of Guinea SSTs are often associated with reduced Sahel rainfall as the monsoon circulation is shifted equatorward and rainfall over the Guinean coast increases (Janicot, 1992; Vizy and Cook, 2002). If similar processes that act on interannual time-scales were important on decadal time-scales, the small warming in the Gulf of Guinea would act to reduce rainfall in the Sahel, but this is not observed here (Figure 2). This suggests that the SSTs in regions outside the Gulf of Guinea are more influential for decadal Sahel rainfall variability.

The second region of SST changes associated with the AMO, the Mediterranean Sea, shows larger SST changes than the Gulf of Guinea, particularly in spring and summer, with significant differences between warm and cold AMO phases of 0.5–1 °C. Observational evidence shows a positive correlation between Sahel rainfall and Mediterranean SST (Rowell, 2003) and between the AMO and Mediterranean SSTs (Marullo *et al.*, 2011; Mariotti and Dell'Aquila, 2012). Additional studies using atmospheric GCMs and idealized modelling show that when the Mediterranean Sea is warm (as in the warm phase of the AMO, Figure 3), the West African monsoon circulation is able to penetrate farther northwards due to increased southward moisture transport and strengthening of the Sahara heat-low (Rowell, 2003; Peyrillé *et al.*, 2007; Fontaine *et al.*, 2010; Gaetani *et al.*, 2010). Hence, the influence of the warm Mediterranean SSTs during the warm phase of the AMO would be expected to oppose the influence of the Gulf of Guinea and act to increase Sahel rainfall.

The third region relating SST to Sahel rainfall is the interhemispheric SST gradient across the Atlantic. As seen in previous studies of Sahel wet and dry periods, an increase in SST in the North Atlantic and little to no change in the South Atlantic (Figure 3) increases the interhemispheric SST gradient which consequently acts to change the SLP gradient and increase the cross-equatorial monsoon flow and Sahel rainfall (Lamb, 1978a, 1978b; Folland *et al.*, 1986; Hastenrath, 1990; Rowell *et al.*, 1995; Ward, 1998; Knight *et al.*, 2006; Zhang and Delworth, 2006; Ting *et al.*, 2009). This mechanism may be acting in conjunction with the increased Mediterranean SSTs in the case of the warm phase of the AMO. Changes in circulation patterns and atmospheric variables will be investigated next to determine the importance of each of these regions during different phases of the AMO, which will improve our understanding

of decadal variability in the region and may prove useful in assessment of GCM simulations of the West African monsoon.

3.2. Surface variables

The same compositing analysis for the SSTs was performed on precipitation from GPCP and CRU and is shown in Figure 4. There is consistency between the GPCP and CRU datasets in the spatial patterns of rainfall differences over Africa (as for the differences in the annual cycle of Sahel rainfall in Figure 2). While spatial patterns are similar, the magnitude of the rainfall difference between warm and cold AMO phases is larger, and more regions show significance in the CRU data than in the GPCP data, which may be a result of the larger sample size in the former.

A significant reduction in rainfall is observed during the warm AMO over much of the North Atlantic midlatitude storm track (from off the east coast of North America to Iceland) throughout the annual cycle. The rainfall reduction in the storm tracks is strongest in winter and spring, and is consistent with a weaker subtropical high and reduced meridional SLP and temperature gradients (See Figs. 5 and 6 discussed later in this section). Over the tropical Atlantic, particularly in spring (Figure 4(b)) and summer (Figure 4(c)), the northern fringe of the ITCZ has increased rainfall during AMO warm phases and the southern fringe has reduced rainfall, consistent with previous studies (Folland *et al.*, 1986; Rowell *et al.*, 1995; Knight *et al.*, 2006; Zhang and Delworth, 2006; Ting *et al.*, 2009). Rainfall increases in the warm phase are also seen in both GPCP and CRU over northeast Brazil (Knight *et al.*, 2006) in spring (Figure 4(b) and (f)) and the Caribbean in summer/autumn (Figure 4(c), (d), (g) and (h)). Changes in the Caribbean may be connected to the increase in hurricane activity during the warm phase of the AMO (Goldenberg *et al.*, 2001; Klotzbach and Gray, 2008).

Areas of significant rainfall increases during warm AMO years are first observed over West Africa in AMJ (as seen in Figure 2, these increases are strongest in June), and are more significant in the CRU data (Figure 4(f)) than GPCP (Figure 4(b)). The significant increased rainfall across the Sahel during warm phases of the AMO is largest (both spatially and in magnitude) during the summer months (as in Figure 2), and is clearly seen in both Figure 4(c) and (g) extending zonally across much of the Sahelian belt. The rainfall across parts of the Sahel (including parts of Chad, Senegal and Mauritania) is in excess of 1.5 mm day^{-1} (or close to 100% of the annual mean rainfall) greater in warm phases of the AMO than cold phases. As the monsoon weakens in autumn, the rainfall increase during warm phases of the AMO is only significant along the Gulf of Guinea coast, with CRU (Figure 4(h)) showing more significant values than GPCP (Figure 4(d)).

Along the Gulf of Guinea coast of central Africa, a significant drying is seen during spring over land in the GPCP data (Figure 4(b)) but not in the CRU data (Figure 4(f)). During summer (Figure 4(c) and (g)), a weak drying signal is observed along the Guinea coast of West Africa in both the GPCP and CRU data. This dipole between the Sahel and Gulf of Guinea coast has some similarities with the dipole mode often seen on interannual time-scales, which is forced by SST changes in the Gulf of Guinea (Nicholson and Webster, 2007). However, SST warming in the Gulf of Guinea and drying near the coast are weak (not significant) suggesting this mechanism is not a leading factor in the AMO impact on the Sahel. Thus, the remainder of the discussion will focus on the explanations for the significant rainfall increase during warm phases of the AMO over the Sahel.

Changes in SLP between warm and cold phases of the AMO are shown in Figure 5. Midlatitude and subtropical SLP changes are largest during winter with reduced pressure during the warm phase of the AMO. Over the subtropical high in winter, SLP differences exceed 3 hPa. Changes in SLP over the North Atlantic are consistent with the modelling work of Grosfeld *et al.* (2008), who show that North Atlantic SLP and SST are in phase at multidecadal time-scales. The weakening of the subtropical high in the Northern Hemisphere and extension of low SLP across northern Africa (SLP reductions of up to 2 hPa during JAS) during the warm phase of the AMO occur throughout the annual cycle and lead to a reduction of the SLP gradient between hemispheres. In the Southern Hemisphere, the subtropical high strengthens during warm phases of the AMO throughout the annual cycle, which contributes to the increased interhemispheric SLP gradient. The significant lowering of SLP over the Sahara is consistent with a deepening (or strengthening) of the Sahara heat-low, which is known to impact the West African monsoon (Lavaysse *et al.*, 2009).

The strengthening of the heat-low is also evident in the surface air temperature difference composites shown in Figure 6. Surface air temperature pattern changes across the Atlantic, Mediterranean and Gulf of Guinea are consistent with the SSTs shown in Figure 3 and remain quite constant throughout the annual cycle, with warming in the North Atlantic much larger than cooling in the South Atlantic. In conjunction with the reduced SLP, surface air temperatures over North Africa are more then 1 °C warmer during the warm phase of the AMO than the cold phase. Warming of North Africa compared to the Gulf of Guinea increases the meridional thermal gradient across the continent which can lead to a strengthening of the monsoon circulation and an increase in Sahel rainfall during summer, as shown in Figure 5(c). Significant cooling in the warm phase of the AMO during spring and summer (Figure 6(b) and (c)) in the Sahel is a result of increased precipitation. The same analysis was performed with the longer time series of land-only surface temperature from the CRU dataset (not shown), and the warming of the Sahara is also evident in these data, supporting the results presented from the re-analysis.

The low-level (925 hPa) winds associated with the difference between the warm and cold phases of the AMO are shown in Figure 7. The enhancement of onshore westerly and onshore southerly wind anomalies during warm phases of the AMO in West Africa is clearly evident throughout the seasonal cycle. Both the westerly and southerly wind increases affecting West Africa have connections to the South Atlantic. In all seasons, the southerly flow through the Gulf of Guinea that reaches the Sahel begins close to 30°S. Similarly, the westerly winds have a southerly component from the South Atlantic that turns eastward as it crosses the Equator and a westerly component from the weakening of the North Atlantic high.

The impact of the warm Mediterranean during warm phases of the AMO is seen predominantly through winter, spring and summer (Figure 7(a)–(c)), with enhanced northeasterly winds originating in the region of the eastern Mediterranean and predominantly influencing the central

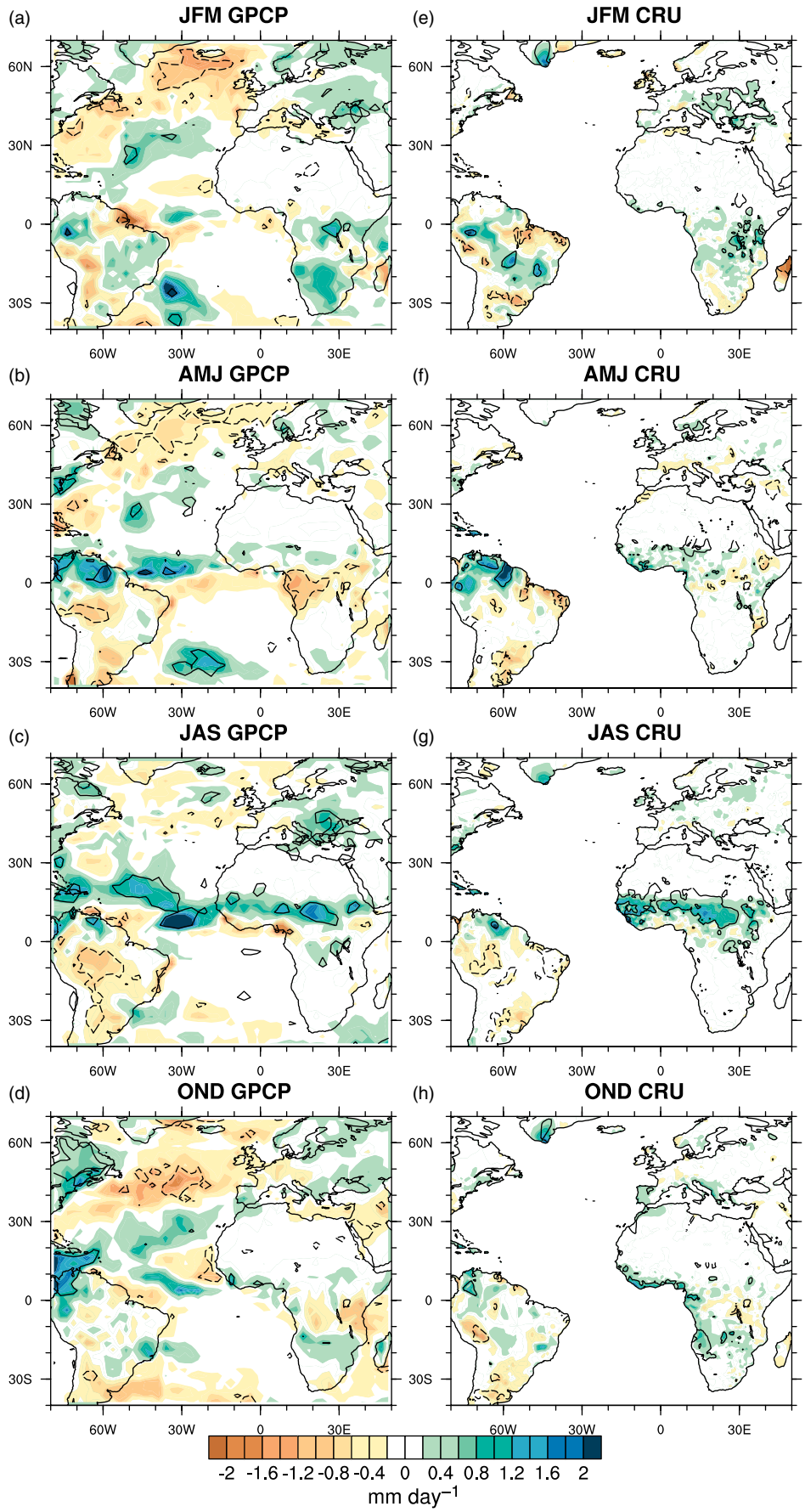

Figure 4. Difference in precipitation (mm day^{-1}) between warm and cold AMO phases from GPCP (left column) and CRU (right column) data. Seasons shown are (a), (e) JFM, (b), (f) AMJ, (c), (g) JAS and (d), (h) OND. Black lines indicate regions where precipitation in warm AMO and cold AMO years are statistically different from each other at the 95% confidence level using a simple Student's *t*-test. Solid lines indicate significant positive differences and dashed lines show significant negative differences. This figure is available in colour online at wileyonlinelibrary.com/journal/qj

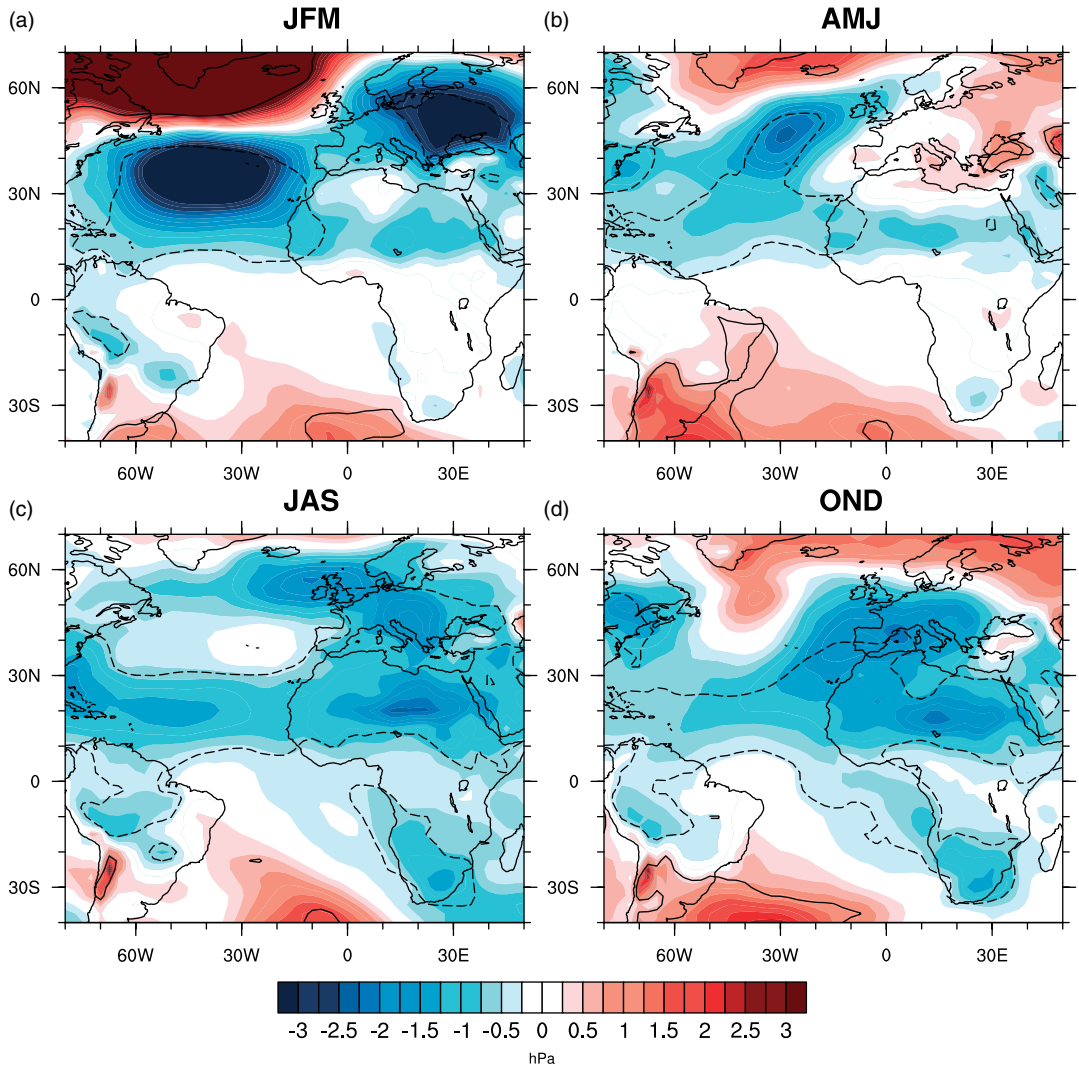

Figure 5. Difference in sea-level pressure (hPa) between warm and cold AMO phases for (a) JFM, (b) AMJ, (c) JAS and (d) OND from NCEP/NCAR re-analysis (1948–2009). Black lines indicate regions where SLP in warm AMO and cold AMO years are statistically different from each other at the 95% confidence level using a simple Student's *t*-test. Solid lines indicate significant positive differences and dashed lines show significant negative differences. This figure is available in colour online at wileyonlinelibrary.com/journal/qj

Sahel. In conjunction with the increased northeasterly winds, the increased specific humidity (not shown) and surface temperatures (Figure 6) lead to an increase in moisture and heat fluxes from the Mediterranean towards the Sahel. This increase in moisture fluxes early in the year may build up moisture in the Sahel prior to the monsoon season that could result in additional rainfall when sufficient forcing for rainfall arrives during the summer months (a full moisture budget analysis would be necessary to confirm this, but is outside the scope of this study). This pattern is consistent with observational studies based on warm and cold Mediterranean SSTs (Gaetani *et al.*, 2010) and modelling output forced only by varying Mediterranean SSTs (Rowell, 2003; Gaetani *et al.*, 2010). Moisture flux convergence in the Sahel through the annual cycle is discussed further in section 5.

4. Annual cycle of rainfall and winds

The patterns of surface variables discussed in section 3.2 indicate significant changes in rainfall, SLP, surface air temperature and low-level winds over West Africa and the surrounding regions throughout the annual cycle. This section will present zonal mean circulation responses to changes in phase of the AMO, and connect these changes with the surface changes already identified. Figure 8 shows the annual cycle (averaged over the Sahel, between 20°W and 10°E) of the warm minus cold phase of the AMO composited rainfall and low-level (925 hPa) winds. Consistent with Figure 2, the increase in precipitation over the Sahel begins in June, with the largest changes at 12°N. The rainfall difference between warm and cold AMO phases maximizes in August and decreases rapidly until October (as seen in Figure 2). Rainfall differences between warm and cold phases of the AMO are above 1 mm day^{-1} during August and September between 10°N and 15°N.

Increased rainfall in June might be expected to be associated with an earlier monsoon onset date, a more intense monsoon or a combination during warm phases of the AMO and should be explored in future work. Evidence from Le Barbé *et al.* (2002) and Sultan and Janicot (2003) suggest little difference in onset date between decadal wet and dry periods; however, differences in methodology, time periods and data exist between the two studies. A single analysis using long-term daily data covering warm and cold

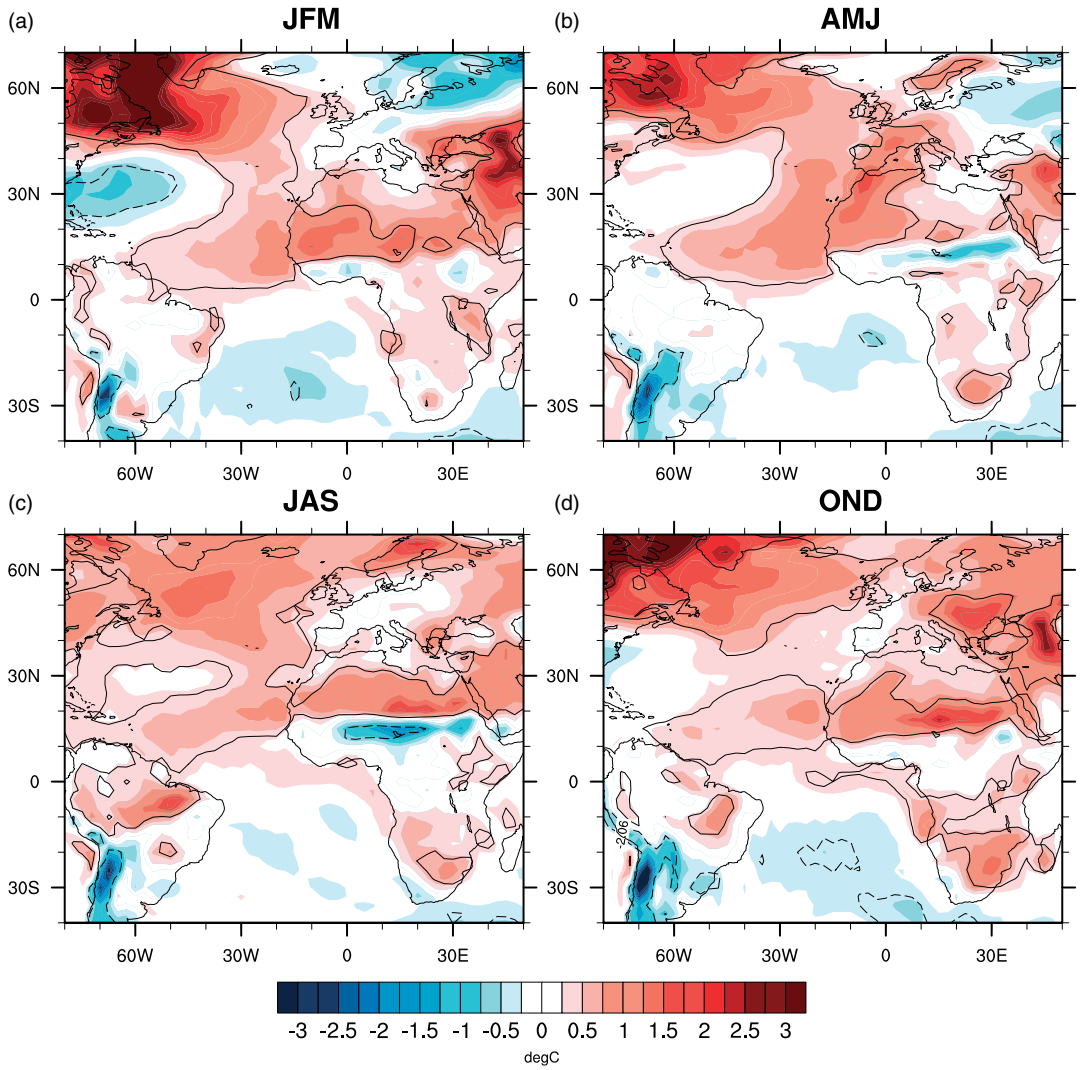

Figure 6. Same as Figure 5 but for surface air temperature (°C). This figure is available in colour online at wileyonlinelibrary.com/journal/qj

phases of the AMO is required to determine the AMO impact on the monsoon onset.

Rainfall deficits over the Gulf of Guinea begin in March close to the Equator and move northward, maximizing just south of the Guinea coast during July despite significantly warmer SSTs there in the warm phase of the AMO (Figure 3). However, the drying over the ocean and coast is not statistically significant, as shown in Figure 4.

Figure 8 also shows the stronger low-level monsoon flow in the warm phase of the AMO compared to the cold phase, as observed in Figure 7. Low-level southerly winds over the Gulf of Guinea, originating south of the Equator, and westerly winds over the Atlantic are increased throughout the entire annual cycle, consistent with increased rainfall in the Sahel. The largest changes in low-level wind speed occur at 10°N, begin in March and increase throughout summer, reaching a maximum in September, a month after the strongest rainfall differences. These wind increases, along with increases in specific humidity at low levels (not shown), act to increase the moisture flux into the Sahel region (section 5) from the west, south and north. The increase in westerly winds from the Atlantic maximizes at 850 hPa throughout the annual cycle and increases in depth from 700 hPa in winter to 400 hPa during summer (not shown). The increase in the westerly and southerly low-level flow into the Sahel is consistent with studies of interannual variability of wet and dry years in the Sahel (e.g. Nicholson and Webster, 2007) despite the different compositing technique used (SST versus rainfall) and the different time period investigated. The increased northeasterly winds from the Mediterranean seen over the eastern Sahara are less evident in this zonal mean than the map in Figure 7 (due to averaging only over the western Sahel); however, small increases in northerly winds are seen across the Sahara during the summer months.

Changes in circulation are not only apparent at low levels. Changes in mid-level winds at 700 hPa are also evident between the warm and cold phases of the AMO. Figure 9 shows the composites of wind speed and direction at 700 hPa (the approximate level of the AEJ during summer) for the warm (Figure 9(a)) and cold (Figure 9(b)) phases of the AMO. Easterly winds are seen in both warm and cold phases throughout the annual cycle, with the summertime AEJ evident in both warm and cold phases of the AMO and reaching its maximum northward position during August. Easterly winds south of 10°N are stronger during the cold phase of the AMO throughout the annual cycle. Latitudinal changes in the AEJ position during summer between the two AMO phases are more apparent than intensity changes, with the AEJ further north during the warm phase of the AMO

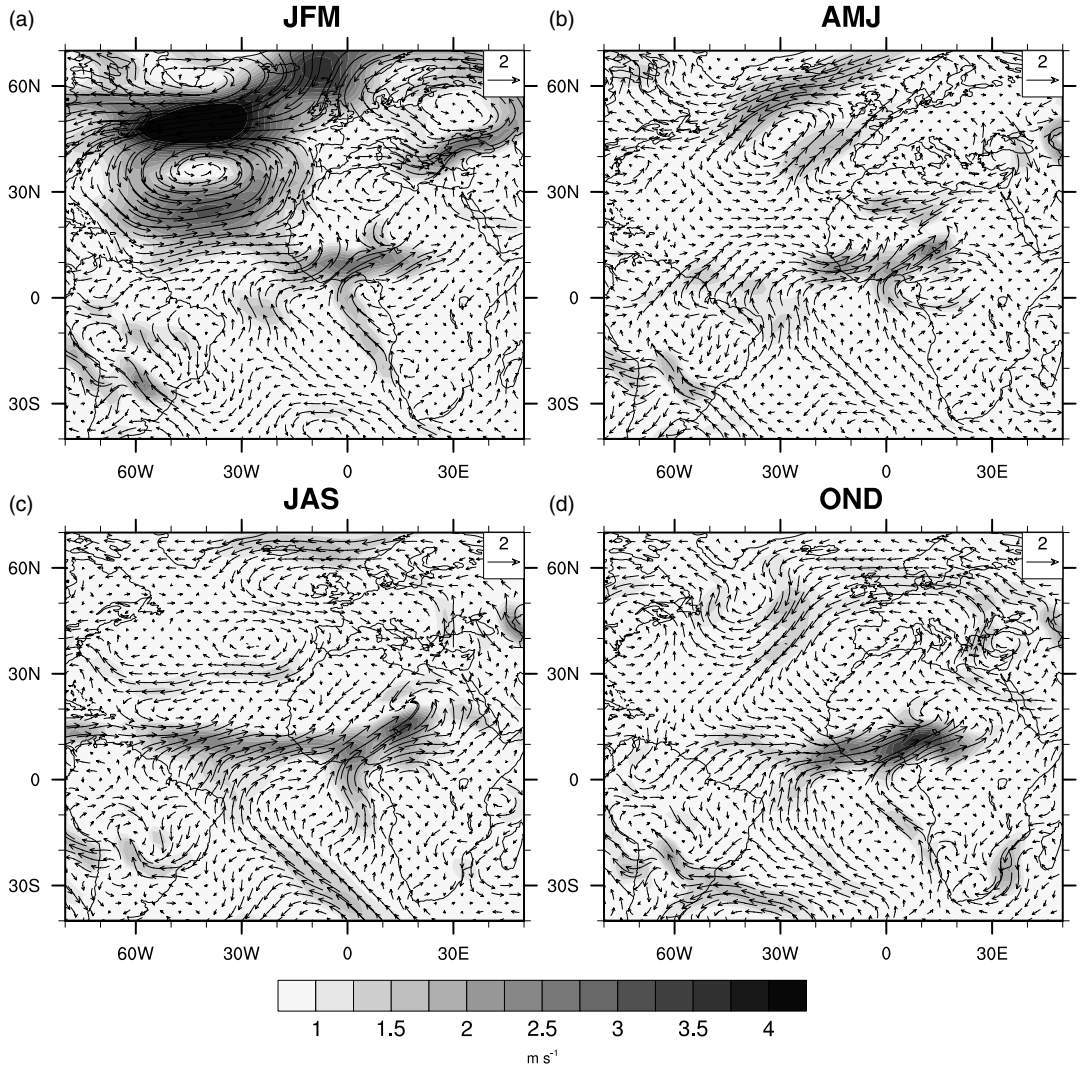

Figure 7. Same as Figure 5 but for 925 hPa wind speed (shading, m s^{-1}) and direction (vectors).

(Figure 9(a)), consistent with the more northerly position of rainfall over the Sahel.

5. Moisture fluxes

Changes in the circulation associated with the warm phase of the AMO, as discussed in section 4, impact moisture transport and rainfall patterns in the region. Specific humidity increases are observed in the warm phase of the AMO throughout the annual cycle below 500 hPa. Increases in humidity are observed as far north as 20°N in spring and 35°N in the summer (not shown), consistent with the increased rainfall over the Sahel and stronger monsoon circulation shown earlier. To diagnose changes in the meridional overturning circulation and moisture flux convergence, seasonal mean north–south cross-sections (averaged between 20°W and 10°E) are shown in Figure 10. The large-scale features are consistent with ECMWF Re-Analysis (ERA) Interim and Modern Era Retrospective analysis for Research and Applications (MERRA) re-analyses shown in Thorncroft *et al.* (2011), despite the resolution differences between the re-analyses. Most notably, the vertical dipole of moisture flux divergence overlying convergence, a signature of the heat-low shallow meridional circulation, is visible throughout the annual cycle and moves northward to 18°N during summer (Figure 10(c)). The weak moisture flux convergence peak near 10°N during summer at 700 hPa that Thorncroft *et al.* (2011) attribute to the shallow meridional circulation is also evident in the National Centers for Environmental Prediction/National Center for Atmospheric Research (NCEP/NCAR) re-analysis. The small-scale features of the NCEP/NCAR re-analysis are most similar to the MERRA re-analysis, with weaker low-level moisture flux divergence separating the coastal and Sahel moisture flux convergence peaks.

The differences between the meridional circulation and moisture flux convergence in the warm and cold phases of the AMO are shown in Figure 11. In winter (Figure 11(a)), a northward shift of the vertical moisture convergence dipole during the warm phase of the AMO compared to the cold phase is evident, with anomalies largest at 11°N. In conjunction with this northward shift in low-level moisture convergence and enhanced cross-equatorial southerly flow, increased moisture divergence is seen at the coast during warm phases of the AMO.

Between winter and spring the peak in mean low-level moisture flux convergence and mid-level moisture flux divergence moves northward to the central Sahel (Figure 10(b)). In the warm phase of the AMO, the vertical dipole associated with the heat-low shallow meridional

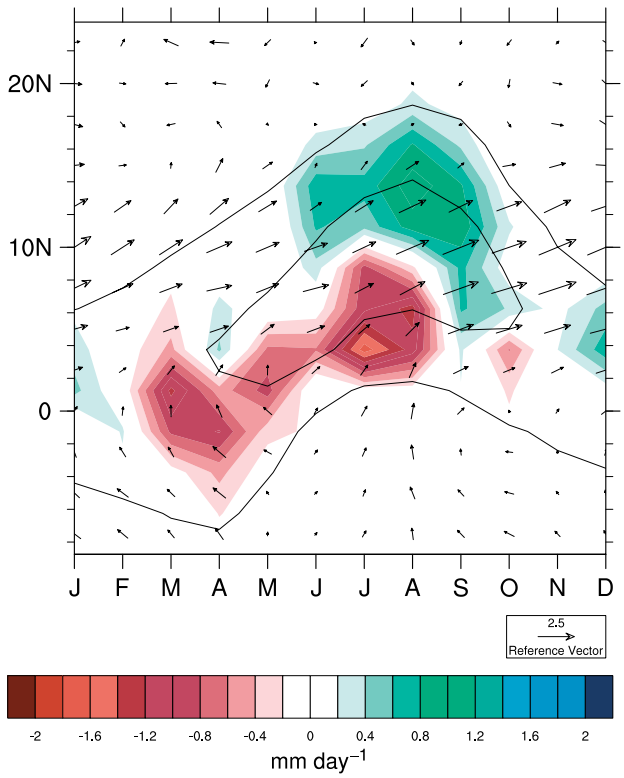

Figure 8. Annual cycle (averaged between 20°W and 10°E) of difference in precipitation (shading, mm day^{-1}) from GPCP and 925 hPa wind vectors from NCEP/NCAR re-analysis between warm and cold AMO years. Solid contours indicate GPCP mean 1 mm day^{-1} and 6 mm day^{-1} precipitation boundaries. This figure is available in colour online at wileyonlinelibrary.com/journal/qj

circulation is northward of its mean location in spring (Figure 11(b)) and a clear enhancement in the cross-equatorial shallow overturning circulation is evident. Vertical motion in the Sahel, mid-level cross-equatorial return flow (at approximately 600 hPa), descent close to 5°S and the low-level southerly return flow are also enhanced in the warm phase of the AMO compared to the cold phase. The enhancement in the southerlies is unlikely to be due to the cold tongue in the Gulf of Guinea (Zheng *et al.*, 1999), as Gulf of Guinea SSTs are warmer during the warm phase of the AMO (Figure 3(b)). The increased cross-equatorial southerly winds on the eastern side of the basin which increases moisture fluxes into the Sahel during the warm phase of the AMO are postulated to be due to the strengthening of the heat-low (section 3.2) and associated shallow meridional circulation (Zhang *et al.*, 2008).

The summer mean conditions (Figure 10(c)) show the vertical dipole in mean moisture flux convergence peak has continued its propagation northward to 18°N. The difference between the warm and cold phases of the AMO shows a large peak in anomalous moisture flux convergence centred at 18°N. The enhancement of low-level moisture flux convergence during the warm phases of the AMO is strongest below 850 hPa, but extends up to 500 hPa, with an equatorward tilt, in conjunction with increased vertical motion. The mean mid-level moisture flux divergence at 20°N is slightly enhanced during the warm phase of the AMO compared to the cold phase. The reduced precipitation observed at the coast (5°N) in the warm phase during summer coincides with increased moisture divergence just above the surface. Increased southerly cross-equatorial winds during summer extend from near 30°S, consistent with increased descent and higher SLP in the South Atlantic (Figure 5), rather than the shallow overturning heat-low circulation seen in spring (Figure 11(b)). Also observed are increased low-level northerly winds to the north of the Sahel during the warm phase of the AMO. Although the increase in northerly winds is weaker than the increased southerly winds to the south of the Sahel (consistent with increased inertial stability), they still contribute to increased southward moisture (and heat) fluxes across the Sahara and into the Sahel, reinforcing the increased precipitation.

In autumn (Figure 10(d)), the mean low-level moisture flux convergence maximum moves southward and weakens as the cross-equatorial southerly flow weakens. Compared to the mean, the low-level moisture flux convergence is once again shifted northward during the warm phase of the AMO (Figure 11(d)). Figures 10 and 11 combine to show that the shallow meridional circulation and moisture flux convergence pattern associated with the heat-low are enhanced during the warm phase of the AMO throughout the annual cycle. Maximum enhancement occurs during spring, prior to the onset of the monsoon, further indicating that the AMO may play a role in the onset date and intensity of the monsoon.

6. African easterly waves

While changes in the large-scale climate, as previously discussed, give insight into the processes controlling the large-scale changes in Sahel precipitation during warm and cold phases of the AMO, analysis of smaller scales is needed to further diagnose changes in rainfall. During the summer, when rainfall changes are largest, synoptic-scale rainfall activity in the Sahel is dominated by African easterly waves (AEWs) (e.g. Carlson, 1969; Kiladis *et al.*, 2006). AEWs are westward-moving mixed baroclinic–barotropic disturbances that arise through interactions between convection and the AEJ (Burpee, 1972; Thorncroft *et al.*, 2008). Increased vertical and horizontal shear of the AEJ during warm phases of the AMO (section 4) increases the instability of the jet that may act to encourage more development of AEWs during warm AMO phases.

As in many previous studies, AEW activity is diagnosed using the eddy kinetic energy (EKE) as follows:

$$EKE = \frac{u'^2 + v'^2}{2} \qquad (1)$$

where the primes indicate 2–10-day filtered anomalies. Four times daily NCEP/NCAR re-analysis was used for the calculation of EKE, with warm and cold phases of the AMO selected in the same way as described for the monthly data in section 2.

The seasonal difference maps for EKE at 700 hPa between warm and cold phases of the AMO are shown in Figure 12. Maximum differences in EKE over West and central Africa are observed during summer (Figure 12(c)), although some small but significant increases are seen over central Africa in spring (Figure 12(b)). Increases in EKE are consistent with the locations of the climatological mean EKE position off the coast of West Africa but a secondary maximum is also noted close to Lake Chad. Similar results are observed for the location of EKE increases at 850 hPa (not shown). In addition to the enhancement during summer, increased

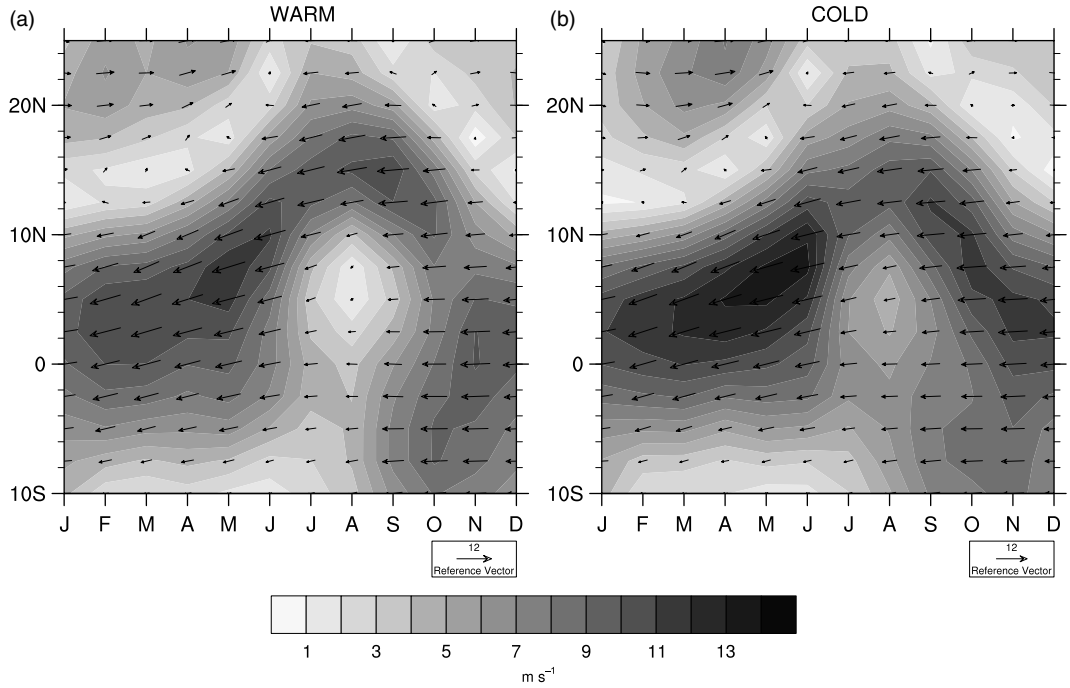

Figure 9. Annual cycle (averaged between 20°W and 10°E) of wind speed (shading, m s^{-1}) and direction (vectors) at 700 hPa for (a) warm AMO phases and (b) cold AMO phases from NCEP/NCAR re-analysis.

EKE in the Sahel and south of the AEJ is also observed in autumn (Figure 12(d)), particularly in October (not shown).

To further examine the annual cycle of EKE and AEW activity over West Africa, the annual cycle of the vertical profile of EKE over West Africa (5°N–20°N, 25°W–5°W) is shown in Figure 13. A large increase in EKE during warm phases of the AMO is seen at mid-levels from June through to November. The largest and most significant increases in EKE over West Africa are observed in June and September at 600 hPa. Regional increases in EKE during the summer months are large and significant at 850 hPa (although not significant in the area-averaged vertical profile in Figure 13). This is in contrast to Grist (2002) who used a compositing technique involving wet and dry years and found enhanced mid-level wave activity during wet Sahel years but little difference at low levels. The large increase in EKE during warm AMO years beginning in June would be expected to impact the frequency of tropical cyclone formation off the coast of West Africa, given a favourable large-scale environment.

The increase in EKE activity is most likely due to more vigorous convection within the AEWs, as seen by the increased precipitation shown in Figure 4. Additional contributions to the increased EKE and AEW activity may be from increased convective triggering of waves and increased instability of the AEJ (Leroux and Hall, 2009; Leroux *et al.*, 2010). During the warm phase of the AMO, increases in vertical and horizontal wind shear in and south of the AEJ core as well as an increased surface air temperature gradient are observed (Figures 6, 8 and 9), which may be acting to increase the instability of the AEJ. In addition to the enhanced convection in the warm phase of the AMO, increased AEJ instability may also play a role in the increased EKE and AEW activity during warm phases of the AMO, but separating these two contributions is beyond the scope of this study.

This increase of EKE and associated AEW activity could have a strong impact on tropical cyclones in the Atlantic. Several studies have shown a link between the warm phase of the AMO and increased tropical cyclones in the Atlantic (Goldenberg *et al.*, 2001; Knight *et al.*, 2006), which has been attributed to increased SSTs and decreased vertical wind shear (Goldenberg *et al.*, 2001; Aiyyer and Thorncroft, 2011) during the warm phase of the AMO. As AEWs are often precursors of tropical depressions and cyclones (e.g. Avila and Pasch, 1992; Thorncroft and Hodges, 2001), this enhancement of AEW activity during the warm phase of the AMO, particularly the increases observed off the coast of West Africa (Figures 12(c) and 13), is suggested to be an additional potential cause of the increased tropical cyclone activity during the warm phase of the AMO (Hopsch *et al.*, 2007). Previous studies (e.g. Xie *et al.*, 2005) have suggested that AEW activity could be modulated by the AMO, but this study explicitly shows an increase in AEWs during the warm phase of the AMO.

The genesis locations, defined as the location where tropical depression wind speed is reached and obtained from the North Atlantic HURricane DATabase (HURDAT: Landsea *et al.*, 2004) of tropical storms during warm and cold phases of the AMO are shown in Figure 14. As expected from previous work, a larger number of storms per year are observed during warm AMO years (13.1) compared to cold AMO years (7.9). Although Kossin and Vimont (2007) show no correlation between the AMO index and mean genesis longitude of tropical storms, it is evident from visual inspection of Figure 14 that more storms formed closer to Africa in the warm phase of the AMO (Figure 14(a)) and more storms formed off the southeast USA in cold phases of the AMO (Figure 14(b)). However, as fewer storms also formed in the Caribbean during cold phases of the AMO, this results in no significant change in the mean longitude (59°W in warm phases of the AMO and 63°W in cold phases of the AMO). It is important to note, however, that the

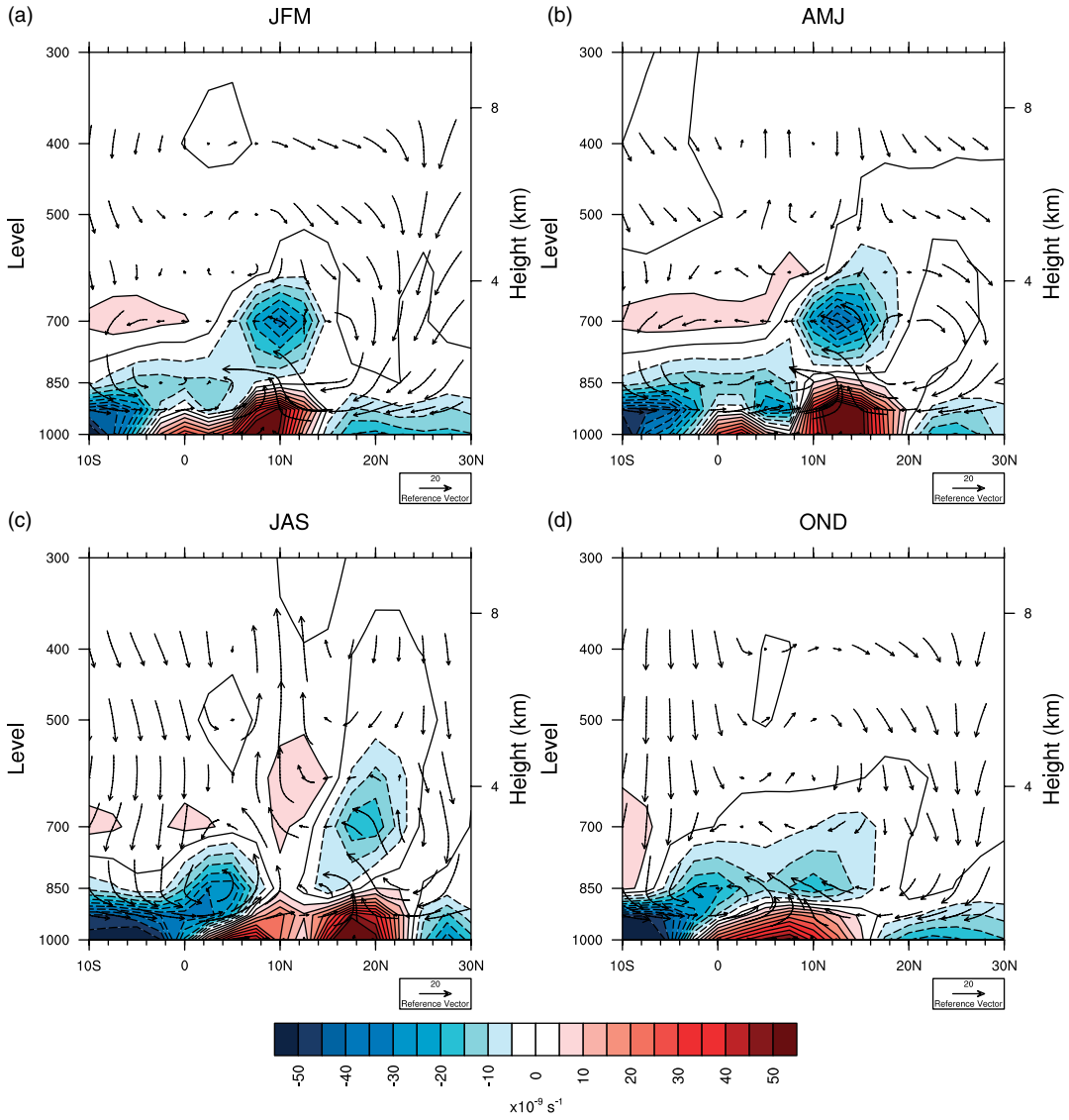

Figure 10. Meridional cross-section (averaged between 20°W and 10°E) of the seasonal mean in moisture flux convergence (shading and contour lines, s^{-1}) and meridional circulation (vectors) for (a) JFM, (b) AMJ, (c) JAS and (d) OND from NCEP/NCAR re-analysis. Solid contours indicate regions of positive moisture flux convergence and dashed contours regions of negative moisture flux convergence. This figure is available in colour online at wileyonlinelibrary.com/journal/qj

relative roles of increased SST, AEW activity and decreased vertical shear during the warm phase of the AMO have not been determined in this study.

7. Summary and discussion

By using a combination of observations and NCEP/NCAR re-analysis, the differences between warm and cold phases of the AMO through the annual cycle over West Africa have been diagnosed. This analysis uses a compositing method based on SST in the North Atlantic rather than the more commonly used method of compositing by wet and dry years in the Sahel.

By presenting composite differences between warm and cold phases of the AMO, it is simple to see the magnitude of the changes between the two periods, which is why this approach was selected. Additional compositing methods using only the tropical Atlantic SST as well as regressing variables onto the AMO index produced results similar to those shown in this study and add support to the use of this methodology.

The well-known increase in summer Sahel precipitation during warm phases of the AMO was observed in both CRU and the shorter GPCP observations, and was shown to begin in spring and peak in summer. In addition to the Sahel rainfall increase, a drying was observed along the Guinea coast and in the Gulf of Guinea. However, this drying was not significant in either the GPCP or longer CRU data but is consistent with increased descent as part of the increased shallow meridional circulation. The timing of the Sahel increase in rainfall and an extended monsoon in the north has major impacts on agriculture, ecology and energy production in the region and further study with higher-resolution rainfall data is required to identify AMO impacts on monsoon onset.

The decreased SLP and increased surface air temperature over the Sahara throughout the annual cycle are consistent with a stronger Saharan heat-low. The shallow meridional circulation associated with the heat-low was shown to be stronger during spring. This cross-equatorial shallow overturning circulation increases southerly winds into the monsoon region during spring, while cross-equatorial flow

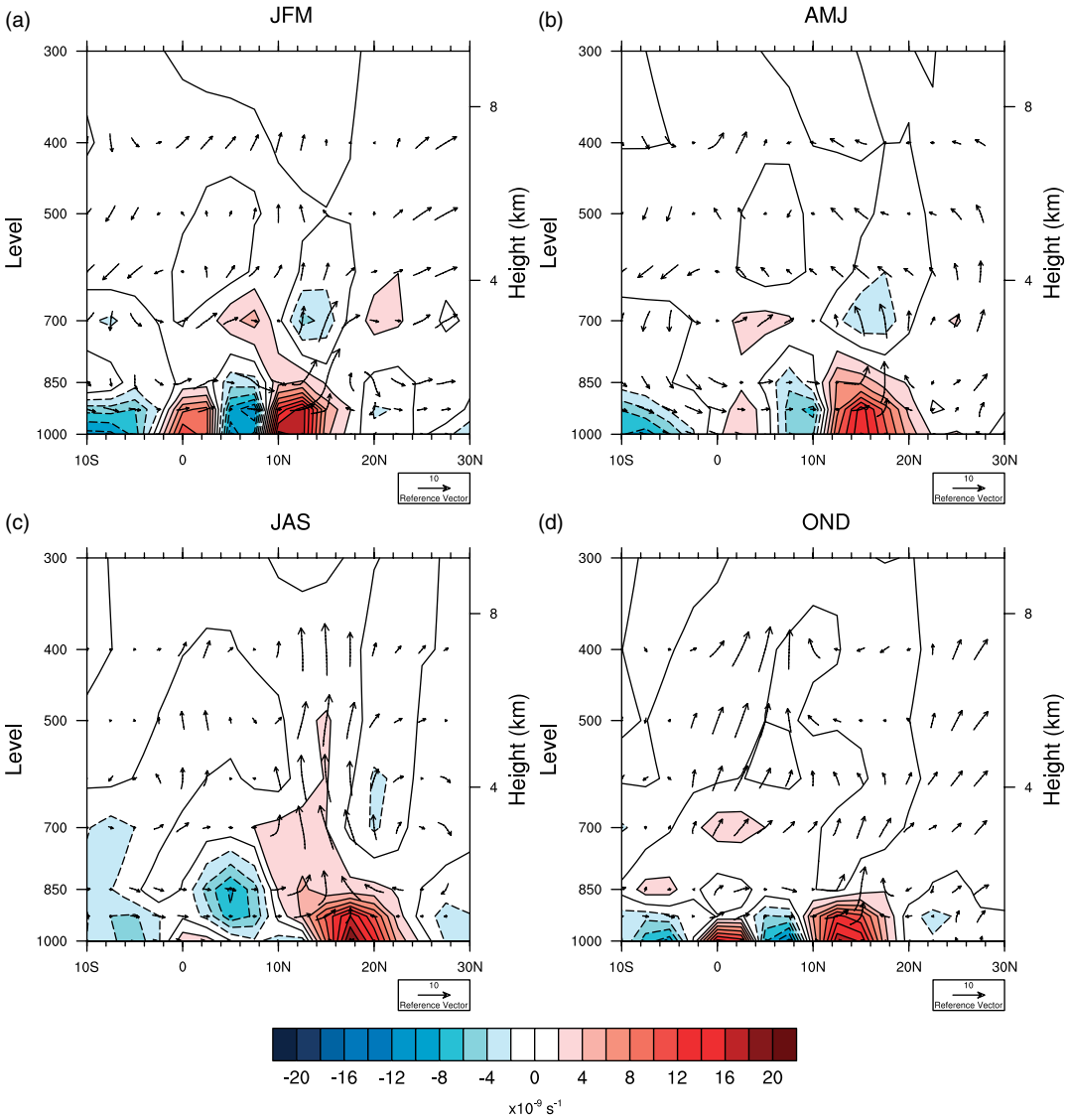

Figure 11. Meridional cross-section (averaged between 20°W and 10°E) of the difference in moisture flux convergence (shading and contour lines, s^{-1}) and meridional circulation (vectors) between warm and cold AMO phases for (a) JFM, (b) AMJ, (c) JAS and (d) OND from NCEP/NCAR re-analysis. Solid (dashed) contours indicate regions where the moisture flux convergence difference between warm and cold AMO years is positive (negative). This figure is available in colour online at wileyonlinelibrary.com/journal/qj

originating from a strong South Atlantic high increases southerly winds through the Gulf of Guinea during summer. This southerly flow in spring and summer increases the moisture flux and associated moisture flux convergence in the region and adds to the northward propagation of the monsoon rains into the Sahel. Biasutti *et al.* (2009) emphasized the connection between the heat-low and Sahel rainfall on interdecadal time-scales in global climate models. The results of this study indicate, for the first time, that the phase of the AMO may control the strength of the heat-low on these decadal time-scales, particularly during spring, and it is suggested that the changes in the heat-low are a major part of the AMO–Sahel rainfall connection.

Changes in the strength of the heat-low are consistent with the warming observed in the Mediterranean during the warm phase of the AMO. According to Rowell (2003), Peyrillé *et al.* (2007), Fontaine *et al.* (2010) and Gaetani *et al.* (2010), a warm Mediterranean Sea increases the monsoonal precipitation over the Sahel in summer by strengthening the heat-low and increasing northeasterly moisture transport toward the Sahel. This study supports the conclusions from these previous studies, but applies them to the time-scales of the AMO and extends them to show that not only do northeasterly winds across the Sahara increase but also southerly winds from the Gulf of Guinea through the impact of the stronger heat-low on the shallow meridional circulation. These wind increases lead to increased moisture flux convergence in the Sahel.

It is important to note that while the meridional circulation strengthens with changes in the heat-low during the warm phase of the AMO, large changes are also observed in the zonal flow at both low and mid levels. Increased westerly winds from the tropical North Atlantic are observed in the warm phase of the AMO, increasing moisture and heat transport into the Sahel. These increased westerly winds arise through the increased interhemispheric SST and SLP gradient (AMO warming is confined to the Northern Hemisphere) in the Atlantic. We suggest that the increased Atlantic interhemispheric SST and SLP gradient during warm phases of the AMO controls the ITCZ northward movement, but over West Africa this mechanism is supplemented by increases in Mediterranean

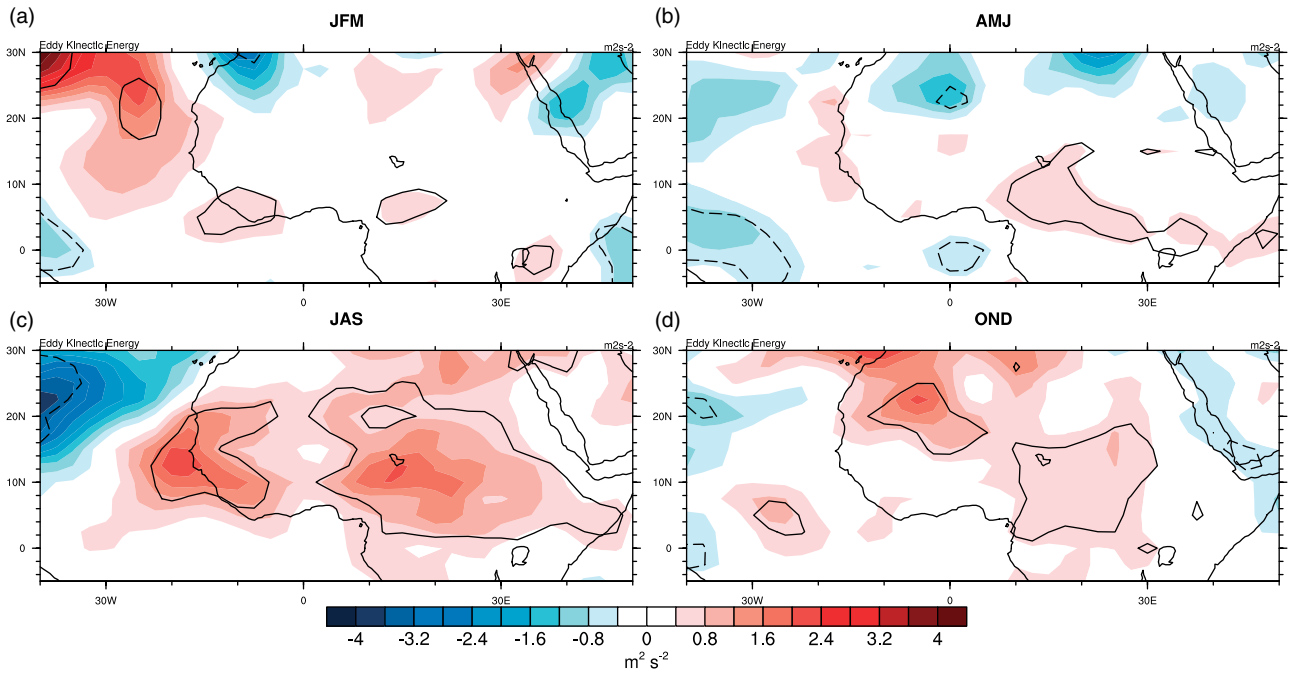

Figure 12. Same as Figure 5 but for eddy kinetic energy ($m^2\ s^{-2}$) from four times daily NCEP/NCAR re-analysis. This figure is available in colour online at wileyonlinelibrary.com/journal/qj

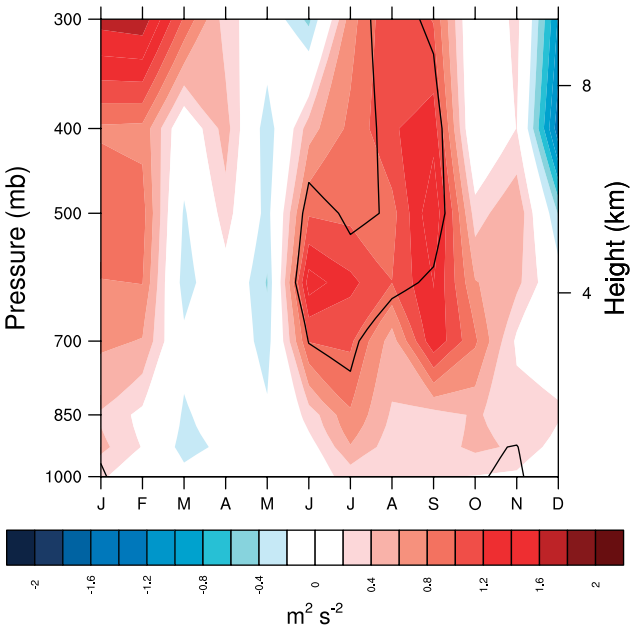

Figure 13. Annual cycle (averaged 25°W–5°W, 5°N–20°N) of the vertical profile of difference in EKE (shading, $m^2\ s^{-2}$) from NCEP/NCAR re-analysis between warm and cold AMO years. Black lines indicate regions where EKE in warm AMO and cold AMO years are statistically different from each other at the 95% confidence level using a simple Student's *t*-test. Solid black lines indicate where this difference is positive. This figure is available in colour online at wileyonlinelibrary.com/journal/qj

SSTs which lead to a stronger heat-low during spring, more shallow overturning, increased moisture convergence and enhancement of the monsoon during summer. A quantitative assessment of the relative roles at decadal timescales of the enhanced moisture flux through westerly winds in the tropical Atlantic, southerly winds in the Gulf of Guinea and northeasterly winds across the Sahara from the Mediterranean requires a full moisture budget which is a potential topic for future study.

At mid-levels, the AEJ is farther north during the summer of warm AMO years. These changes in the low-level westerlies and the AEJ are consistent with changes observed in a small sample of wet and dry years by Grist and Nicholson (2001). Increased vertical and horizontal wind shear associated with the AEJ during the summer of warm phases of the AMO is postulated to be a factor in increased AEW activity during warm phases of the AMO in conjunction with increased rainfall and latent heating within the waves and increased triggering of the waves themselves. Increased EKE is observed across the majority of West Africa during the summer of warm phases of the AMO, with differences between warm and cold phases peaking at 600 hPa during June and September. This increase in AEWs is suggested to be a prominent feature of the increased Sahel rainfall during warm phases of the AMO. A significant increase in EKE is also observed at the West African coast particularly at the beginning and end of the monsoon season, suggesting more AEWs propagating into the Atlantic, and consistent with the increased hurricane activity during warm phases of the AMO (consistent with Hopsch *et al.* (2007)).

Further investigation is required to identify the relative roles of increased AEWs versus increased SST and decreased vertical wind shear for tropical storm development during warm phases of the AMO and is outside the scope of this study. This could partly be addressed by investigating the structure of AEWs in warm and cold phases of the AMO to determine if the increased EKE and AEW activity during warm phases is conducive for increasing tropical cyclogenesis in the Atlantic (i.e. Hopsch *et al.*, 2010).

Acknowledgements

The authors would like to thank the editor, associate editor and two anonymous reviewers for their comments that greatly improved this manuscript. This research was supported by NOAA grant NA10OAR4310205. Monthly

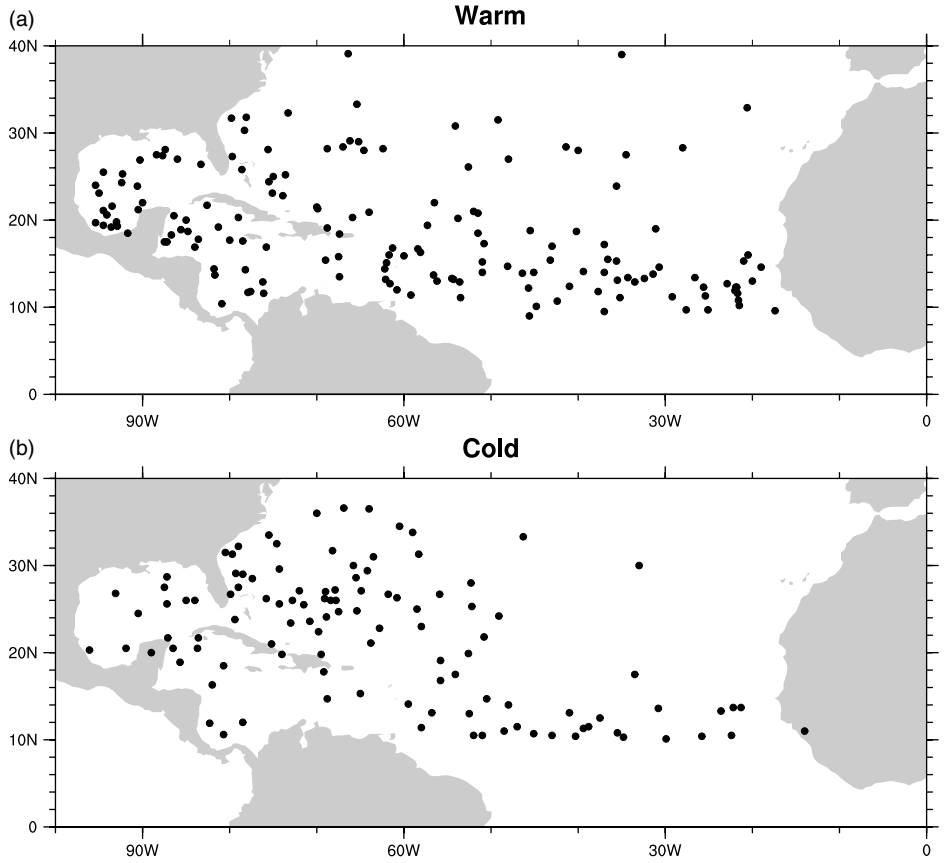

Figure 14. Locations of tropical storm genesis in the Atlantic for (a) warm and (b) cold AMO years from HURDAT.

GPCP combined precipitation data were developed and computed by the NASA/Goddard Space Flight Centers Laboratory for Atmospheres as a contribution to the GEWEX GPCP. NCEP re-analysis data provided by the NOAA/OAR/ESRL PSD, Boulder, CO, USA were obtained from the Web site at http://www.esrl.noaa.gov/psd/. University of East Anglia Climatic Research Unit (CRU) time series high-resolution gridded datasets and Met Office, Hadley Centre HadISST 1.1 - Global sea-Ice coverage and SST were both provided by NCAS British Atmospheric Data Centre at their website http://badc.nerc.ac.uk/.

References

Ackerley D, Booth BBB, Knight SHE, Highwood EJ, Frame DJ, Allen MR, Rowell DP. 2011. Sensitivity of twentieth-century Sahel rainfall to sulfate aerosol and CO_2 forcing. *J. Climate* **24**: 4999–5014.

Adler RF, Huffman GJ, Chang A, Ferraro R, Xie P-P, Janowiak J, Rudolf B, Schieder U, Curtis S, Bolvin D, Gruber A, Susskind J, Arkin P, Nelkin E. 2003. The version-2 Global Precipitation Climatology Project (GPCP) monthly precipitation analysis (1979–present). *J. Hydrometeorol.* **4**: 1147–1167.

Aiyyer A, Thorncroft CD. 2011. Interannual-to-multidecadal variability of vertical shear and tropical cyclone activity. *J. Climate* **24**: 2949–2962.

Avila LA, Pasch RJ. 1992. Atlantic tropical systems of 1991. *Mon. Weather Rev.* **120**: 2688–2696.

Bader J, Latif M. 2003. The impact of decadal-scale Indian Ocean sea surface temperature anomalies on Sahelian rainfall and the North Atlantic Oscillation. *Geophys. Res. Lett.* **30**: 2169, DOI: 10.1029/2003GL018426.

Biasutti M, Held IM, Sobel AH, Giannini A. 2008. SST forcings and Sahel rainfall variability in simulations of the twentieth and twenty-first centuries. *J. Climate* **21**: 3471–3486.

Biasutti M, Sobel AH, Camargo SJ. 2009. The role of the Sahara low in summertime Sahel rainfall variability and change in the CMIP3 models. *J. Climate* **22**: 5755–5771.

Booth BBB, Dunstone NJ, Halloran PR, Andrews T, Bellouin N. 2012. Aerosols implicated as a prime driver of twentieth-century North Atlantic climate variability. *Nature* **484**: 228–232. Erratum **485**: 534.

Burpee RW. 1972. The origin and structure of easterly waves in the lower troposphere of North Africa. *J. Atmos. Sci.* **29**: 77–90.

Caminade C, Terray L. 2010. Twentieth century Sahel rainfall variability as simulated by the ARPEGE AGCM, and future changes. *Clim. Dyn.* **35**: 75–94.

Carlson TN. 1969. Synoptic histories of three African disturbances that developed into Atlantic hurricanes. *Mon. Weather Rev.* **97**: 256–276.

Cook KH, Vizy EK. 2006. Coupled model simulations of the West African monsoon system: Twentieth- and twenty-first-century simulations. *J. Climate* **19**: 3681–3703.

Enfield DB, Mestas-Nuñez AM, Trimble PJ. 2001. The Atlantic multidecadal oscillation and its relation to rainfall and river flows in the continental U.S. *Geophys. Res. Lett.* **28**: 2077–2080.

Folland CK, Palmer TN, Parker DE. 1986. Sahel rainfall and worldwide sea temperatures, 1901–85. *Nature* **320**: 602–607.

Fontaine B, García-Serrano J, Roucou P, Rodríguez-Fonseca B, Losada T, Chauvin F, Gervois S, Sijikumar S, Ruti P, Janicot S. 2010. Impacts of warm and cold situations in the Mediterranean basins on the West African monsoon: Observed connection patterns (1979–2006) and climate simulations. *Clim. Dyn.* **35**: 95–114.

Gaetani M, Fontaine B, Roucou P, Baldi M. 2010. Influence of the Mediterranean Sea on the West African monsoon: Intraseasonal variability in numerical simulations. *J. Geophys. Res.* **115**: D24115, DOI: 10.1029/2010JD014436.

Giannini A, Saravanan R, Chang P. 2003. Oceanic forcing of Sahel rainfall on interannual to interdecadal time scales. *Science* **302**: 1027–1030.

Goldenberg SB, Landsea CW, Mestas-Nuñez AM, Gray WM. 2001. The recent increase in Atlantic hurricane activity: Causes and implications. *Science* **293**: 474–479.

Grist JP. 2002. Easterly waves over Africa. Part I: The seasonal cycle and contrasts between wet and dry years. *Mon. Weather Rev.* **130**: 197–211.

Grist JP, Nicholson SE. 2001. A study of the dynamic factors influencing the rainfall variability in the West African Sahel. *J. Climate* **14**: 1337–1359.

Grosfeld K, Lohmann G, Rimbu N. 2008. The impact of Atlantic and Pacific Ocean sea surface temperature anomalies on the North Atlantic multidecadal variability. *Tellus* **60A**: 728–741.
Hagos SM, Cook KH. 2007. Dynamics of the West African monsoon jump. *J. Climate* **20**: 5264–5284.
Hastenrath S. 1990. Decadal-scale changes of the circulation in the tropical Atlantic sector associated with Sahel drought. *Int. J. Climatol.* **10**: 459–472.
Hastenrath S, Polzin D. 2011. Long-term variations of circulation in the tropical Atlantic sector and Sahel rainfall. *Int. J. Climatol.* **31**: 649–655.
Hopsch SB, Thorncroft CD, Hodges K, Aiyyer A. 2007. West African storm tracks and their relationship to Atlantic tropical cyclones. *J. Climate* **20**: 2468–2483.
Hopsch SB, Thorncroft CD, Tyle KR. 2010. Analysis of African easterly wave structures and their role in influencing tropical cyclogenesis. *Mon. Weather Rev.* **138**: 1399–1419.
Janicot S. 1992. Spatiotemporal variability of West African rainfall. Part II: Associated surface and airmass characteristics. *J. Climate* **5**: 499–511.
Joly M, Voldoire A. 2010. Role of the Gulf of Guinea in the inter-annual variability of the West African monsoon: What do we learn from CMIP3 coupled simulations? *Int. J. Climatol.* **30**: 1843–1856.
Kalnay E, Kanamitsu M, Kistler R, Collins W, Deaven D, Gandin L, Iredell M, Saha S, White G, Woollen J, Zhu Y, Chelliah M, Ebisuzaki W, Higgins W, Janowiak J, Mo KC, Ropelewski C, Wang J, Leetmaa A, Reynolds R, Jenne R, Joseph D. 1996. The NCEP/NCAR 40-year reanalysis project. *Bull. Am. Meteorol. Soc.* **77**: 437–471.
Kerr RA. 2000. A North Atlantic climate pacemaker for the centuries. *Science* **288**: 1984–1985.
Kiladis GN, Thorncroft CD, Hall NMJ. 2006. Three-dimensional structure and dynamics of African easterly waves. Part I: Observations. *J. Atmos. Sci.* **63**: 2212–2230.
Klotzbach PJ, Gray WM. 2008. Multidecadal variability in North Atlantic tropical cyclone activity. *J. Climate* **21**: 3929–3935.
Knight JR, Allan RJ, Folland CK, Vellinga M, Mann ME. 2005. A signature of persistent natural thermohaline circulation cycles in observed climate. *Geophys. Res. Lett.* **32**: L20708, DOI: 10.1029/2005GL024233.
Knight JR, Folland CK, Scaife AA. 2006. Climate impacts of the Atlantic Multidecadal Oscillation. *Geophys. Res. Lett.* **33**: L17706, DOI: 10.1029/2006GL026242.
Kossin JP, Vimont DJ. 2007. A more general framework for understanding Atlantic hurricane variability and trends. *Bull. Am. Meteorol. Soc.* **88**: 1767–1781.
Landsea CW, Anderson C, Charles N, Clark G, Dunion J, Fernandez-Partagas J, Hungerford P, Neumann C, Zimmer M. 2004. The Atlantic hurricane database re-analysis project: Documentation for the 1851–1910 alterations and additions to the HURDAT database. Pp 177–221 in *Hurricanes and Typhoons: Past, present, and future*, Murname RJ, Liu K-B (eds), Columbia University Press.
Lamb PJ. 1978a. Case studies of tropical Atlantic surface circulation patterns during recent sub-Saharan weather anomalies: 1967 and 1968. *Mon. Weather Rev.* **106**: 482–491.
Lamb PJ. 1978b. Large-scale tropical Atlantic surface circulation patterns associated with subsaharan weather anomalies. *Tellus* **30**: 240–251.
Lavaysse C, Flamant C, Janicot S, Parker DJ, Lafore J-P, Sultan B, Pelon J. 2009. Seasonal evolution of the West African heat low: A climatological perspective. *Clim. Dyn.* **33**: 313–330.
Le Barbé L, Lebel T, Tapsoba D. 2002. Rainfall variability in West Africa during the years 1950–90. *J. Climate* **15**: 187–202.
Leroux S, Hall NMJ. 2009. On the relationship between African easterly waves and the African easterly jet. *J. Atmos. Sci.* **66**: 2303–2316.
Leroux S, Hall NMJ, Kiladis GN. 2010. A climatological study of transient–mean-flow interactions over West Africa. *Q. J. R. Meteorol. Soc.* **136**(S1): 397–410.
Lu J. 2009. The dynamics of the Indian Ocean sea surface temperature forcing of Sahel drought. *Clim. Dyn.* **33**: 445–460.
Mariotti A, Dell'Aquila A. 2012. Decadal climate variability in the Mediterranean region: Roles of large-scale forcings and regional processes. *Clim. Dyn.* **38**: 1129–1145.
Marullo S, Artale V, Santoleri R. 2011. The SST multidecadal variability in the Atlantic–Mediterranean region and its relation to AMO. *J. Climate* **24**: 4385–4401.
Mitchell TD, Jones PD. 2005. An improved method of constructing a database of monthly climate observations and associated high-resolution grids. *Int. J. Climatol.* **25**: 693–712.
Mohino E, Janicot S, Bader J. 2011. Sahel rainfall and decadal to multi-decadal sea surface temperature variability. *Clim. Dyn.* **37**: 419–440.
Nicholson SE, Grist JP. 2001. A conceptual model for understanding rainfall variability in the West African Sahel on interannual and interdecadal timescales. *Int. J. Climatol.* **21**: 1733–1757.
Nicholson SE, Webster PJ. 2007. A physical basis for the interannual variability of rainfall in the Sahel. *Q. J. R. Meteorol. Soc.* **133**: 2065–2084.
Okumura Y, Xie S-P. 2004. Interaction of the Atlantic equatorial cold tongue and the African monsoon. *J. Climate* **17**: 3589–3602.
Peyrillé P, Lafore J-P, Redelsperger J-L. 2007. An idealized two-dimensional framework to study the West African monsoon. Part I: Validation and key controlling factors. *J. Atmos. Sci.* **64**: 2765–2782.
Rayner NA, Parker DE, Horton EB, Folland CK, Alexander LV, Rowell DP, Kent EC, Kaplan A. 2003. Global analyses of sea surface temperature, sea ice, and night marine air temperature since the late nineteenth century. *J. Geophys. Res.* **108**: 4407, DOI: 10.1029/2002JD002670.
Rodríguez-Fonseca B, Janicot S, Mohino E, Losada T, Bader J, Caminade C, Chauvin F, Fontaine B, García-Serrano J, Gervois S, Joly M, Polo I, Ruti P, Roucou P, Voldoire A. 2011. Interannual and decadal SST-forced responses of the West African monsoon. *Atmos. Sci. Lett.* **12**: 67–74.
Rowell DP. 2003. The impact of Mediterranean SSTs on the Sahelian rainfall season. *J. Climate* **16**: 849–862.
Rowell DP, Folland CK, Maskell K, Ward MN. 1995. Variability of summer rainfall over tropical north Africa (1906–92): Observations and modelling. *Q. J. R. Meteorol. Soc.* **121**: 669–704.
Shanahan TM, Overpeck JT, Anchukaitis KJ, Beck JW, Cole JE, Dettman DL, Peck JA, Scholz CA, King JW. 2009. Atlantic forcing of persistent drought in West Africa. *Science* **324**: 377–380.
Sultan B, Janicot S. 2003. The West African monsoon dynamics. Part II: The 'preonset' and 'onset' of the summer monsoon. *J. Climate* **16**: 3407–3427.
Thorncroft CD, Hodges KI. 2001. African easterly wave variability and its relationship to Atlantic tropical cyclone activity. *J. Climate* **14**: 1166–1179.
Thorncroft CD, Hall NMJ, Kiladis GN. 2008. Three-dimensional structure and dynamics of African easterly waves. Part III: Genesis. *J. Atmos. Sci.* **65**: 3596–3607.
Thorncroft CD, Nguyen H, Zhang CD, Peyrillé P. 2011. Annual cycle of the West African monsoon: Regional circulations and associated water vapour transport. *Q. J. R. Meteorol. Soc.* **137**: 129–147.
Ting MF, Kushnir Y, Seager R, Li CH. 2009. Forced and internal twentieth-century SST trends in the North Atlantic. *J. Climate* **22**: 1469–1481.
Vizy EK, Cook KH. 2002. Development and application of a mesoscale climate model for the Tropics: Influence of sea surface temperature anomalies on the West African monsoon. *J. Geophys. Res.* **107**: D34023, DOI: 10.1029/2001JD000686.
Wang S-Y, Gillies RR. 2011. Observed change in Sahel rainfall, circulations, African easterly waves, and Atlantic hurricanes since 1979. *Int. J. Geophys.* **2011**: 259529, DOI: 10.1155/2011/259529.
Ward MN. 1998. Diagnosis and short-lead time prediction of summer rainfall in tropical North Africa at interannual and multidecadal timescales. *J. Climate* **11**: 3167–3191.
Xie L, Tingzhuang Y, Pietrafesa L. 2005. The effect of Atlantic sea surface temperature dipole mode on hurricanes: Implications for the 2004 Atlantic hurricane season. *Geophys. Res. Lett.* **32**: L03701, DOI: 10.1029/2004GL021702.
Zhang CD, Nolan DS, Thorncroft CD, Nguyen H. 2008. Shallow meridional circulations in the tropical atmosphere. *J. Climate* **21**: 3453–3470.
Zhang R, Delworth TL. 2006. Impact of Atlantic multidecadal oscillations on India/Sahel rainfall and Atlantic hurricanes. *Geophys. Res. Lett.* **33**: L17712, DOI: 10.1029/2006GL026267.
Zheng XY, Eltahir EAB, Emanuel KA. 1999. A mechanism relating tropical Atlantic spring sea surface temperature and West African rainfall. *Q. J. R. Meteorol. Soc.* **125**: 1129–1163.

